Applied Catalysis A, General 683 (2024) 119860

Contents lists available at ScienceDirect

Applied Catalysis A, General

journal homepage: www.elsevier.com/locate/apcata

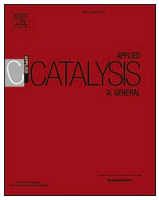

A green and moderate approach for the synthesis of methyl formate via dimethoxymethane disproportionation over H-zeolites

Leilei Yang [a,b], Youming Ni [a], Mingguan Xie [a,b], Zhiyang Chen [a], Xudong Fang [a], Bin Li [a,b], Hongchao Liu [a,*], Wenliang Zhu [a,*]

[a] National Engineering Research Center of Lower-Carbon Catalysis Technology, Dalian Institute of Chemical Physics, Chinese Academy of Sciences, Dalian, Liaoning 116023, China
[b] University of Chinese Academy of Sciences, Beijing 100049, China

ARTICLE INFO

Keywords:
Dimethoxymethane
Methyl formate
Disproportionation
Zeolite
H-SSZ-13

ABSTRACT

Methyl formate (MF) is an important building block in the modern chemical industry, primarily produced through homogeneous carbonylation of methanol under harsh reaction conditions. It is of great interest but remains challenges to develop new heterogeneous catalytic system under mild reaction conditions to replace the homogeneous route. Herein, we report an efficient and green strategy for MF production by dimethoxymethane (DMM) disproportionation over acidic zeolites. Up to nearly100 % DMM conversion and 0.76 g g_{cat}^{-1} h^{-1} of MF space time yield (STY) is achieved over H-SSZ-13 under moderate conditions of 0.1 MPa and 393 K. Moreover, H-SSZ-13 shows superior stability during a 100 h continuous test. Combined with multiple characterizations, formaldehyde (FA) has been proved to be a crucial precursor for the formation of MF and the complete mechanism is proposed. This strategy provides a new and feasible approach for continuous large-scale MF production using acidic zeolite as catalyst by heterogeneous catalytic systems.

1. Introduction

As one of the most important C1 intermediates, methyl formate(MF) is widely employed as feedstock to produce formic acid, dimethyl carbonate, ethylene glycol, methyl acrylate, et al. [1,2]. At present, the liquid-phase methanol (MeOH) carbonylation catalyzed by sodium methoxide is the primary industrial method for MF production, which needs the high pressure and homogeneous catalysts. Unfortunately, some inevitable drawbacks in the process such as severe corrosion, strict reactant purity, low methanol conversion (Table S1) and difficulty in the separation constrain its further development. Although considerable advancement towards catalysts [3–6] and novel production methods have been proposed, the aforementioned constraints still prevent the commercialization of MF synthesis route. Thereinto, more attention has been paid to the alternative synthesis methods, such as dehydrogenation [7,8], oxidative of methanol [9,10], one-step syngas synthesis [11,12] and so on [13–15], as shown in Table S1 - S2. Among these, only methanol dehydrogenation has achieved relatively limited industrial-scare production due to the thermodynamic limitation, whereas others are deficient to achieve the industry practice. Therefore, it is imperative to develop an efficient technology for MF production.

Dimethoxymethane (DMM), produced easily from green methanol or dimethyl ether (DME) [16,17], is widely used for the production of high value-added chemicals, especially for oxygenates. Notably, Bell et al. [18–20] first reported a new production method of methyl methoxyacetate from DMM carbonylation catalyzed by acidic zeolites, and 79 % selectivity was achieved over H-Y zeolite at 393 K and 2 MPa. Subsequently, the reaction has garnered significant attention and interest [21–23]. Interestingly, trace of MF was always observed during the process of DMM carbonylation over solid acid [18,19,24–26], especially for zeolite catalysts. These inspire us to consider whether MF can be produced from DMM.

Acidic zeolites attract much attentions as green solid catalysts due to their unique shape selectivity, tuneable acidity and low production costs [27]. Recently, abundant new reactions and technologies using different zeolites as catalysts have been developed and even commercialized. For example, the world's first MTO plant was started up in 2010 in China using H-SAPO-34 as catalysts [28]. Selective carbonylation of DME to methyl acetate over acidic zeolites was first reported in 2006 [29]. Remarkably, the DME carbonylation reaction has been commercialized

* Corresponding authors.
E-mail addresses: chliu@dicp.ac.cn (H. Liu), wlzhu@dicp.ac.cn (W. Zhu).

https://doi.org/10.1016/j.apcata.2024.119860
Received 16 April 2024; Received in revised form 7 June 2024; Accepted 25 June 2024
Available online 25 June 2024

successfully [30]. Moreover, the process about selective catalytic reduction of NOx with ammonia over SSZ-13 zeolite was developed and implemented [31,32]. These huge progresses achieved in the past decades based on zeolites encourage us to explore its potential capacity for DMM disproportionation.

Herein, we present an efficient and green strategy for MF production from DMM based on methanol/DME over acidic zeolites under moderate conditions, as shown in Fig. 1(a). Specifically, DMM is transformed into MF and DME catalyzed by acidic zeolites. Subsequently, MF could be separated simply from products, and DME which could be directly synthesized by C1 chemicals [33,34], is recycled to produce DMM. Based on this strategy, we first prove that all H-zeolites investigated in this research can efficiently transform DMM to MF. Specifically, nearly 100 % DMM conversion and 0.76 g g_{cat}^{-1} h^{-1} of MF STY could be obtained over H-SSZ-13 at 0.1 MPa and 393 K. Moreover, the H-SSZ-13 shows outstanding stability during the 100 h test. Compared with previous industrial technology, DMM disproportionation circumvents the drawbacks caused by homogeneous catalyst, and displays more sustainable and energy saving, possessing a great potential for continuous large-scale production.

2. Experimental section

2.1. Catalyst information

H-Y, H-SAPO-34, H-ZSM-5, H-ZSM-35, Na-MCM-22, H-SSZ-13 zeolites were purchased from Nankai University Catalyst Ltd. Na-MOR (Si/Al = 13.3) was obtained from YanChang-ZhongKe Catalyst Ltd. Typically, Na-zeolites were treated by ion exchange using 1 M NH_4NO_3 aqueous three times at 353 K followed by filtration and washing with distilled water three times, then dried at 393 K for 24 h and calcined at 823 K for 4 h in air to obtain H-zeolites.

In order to regulate the acid properties of zeolite, the commercial H-SSZ-13 was exchanged by different concentration $NaNO_3$ aqueous solution with mass ratio of 1:10 at 353 K, followed by filtration and washing with deionized water, then dried at 393 K for 10 h. Then the sample was calcined at 823 K for another 4 h in air to obtain a series of x %H-SSZ-13 zeolites ("x" indicates the degree of H^+-exchange, which is determined by 100-(Na/Al) mol% in this work). The detailed information is shown in Table 1.

2.2. Catalyst characterization

The crystallinity of zeolites was characterized by PANalytical X'Pert PRO X-ray powder diffraction using a Cu-Kα (λ = 0.151 nm) radiation source operated at 40 kV and 40 mA. The composition of zeolites was determined by Philips Magix-601 X-ray fluorescence (XRF). The images of zeolites were obtained by a Hitachi SU8020 Scanning Electron Microscopy (SEM) operated at 20 kV. The acidity of zeolites was measured on a Micromeritics Auto Chem 2920 equipped with a TCD. 0.2 g sample was loaded into a U-shaped quartz tube and pretreated on 823 K for 4 h in He. Then, the sample was cooled to 373 K and saturated with NH_3. After removing physically adsorbed NH_3 in He, desorption was performed from 423 K to 923 K at a heating rate of 10 K min^{-1} in He. The textural properties of zeolites with different topology were obtained from N_2 adsorption and desorption using Micromeritics ASAP 2020. Before test, the sample was pretreated at 623 K for 6 h to remove the water. Nitrogen adsorption - desorption isotherms were obtained at 77 K, and the micropore surface area and pore volumes of samples were calculated by the t-plot method.

Table 1
The detailed treatment parameter for H^+ exchange.

Sample	c($NaNO_3$)/ (mol L^{-1})	Exchange times
90.0 %H-SSZ-13	0.1	3
77.4 %H-SSZ-13	2.0	3

2.3. Catalyst test

The conversion of DMM is performed in an atmospheric-pressure fixed-bed flow reactor (inside diameter = 7 mm) made by stainless steel. Typically, a proper amount of the catalyst (20–40 mesh) was loaded into reactor then filled with quartz sand (20–40 mesh). Prior to reaction, the catalyst was first pretreated at 673 K for 3 h with Ar flow (30 mL/min) to remove water in zeolite and reactor and then cooled down to reaction temperature. DMM (0.008 mL/min) was steadily pumped into the reactor by a pump. The results of catalyst evaluation were analyzed by online gas chromatographs (Agilent 7890B), which was equipped with a flame ionization detector (FID). The PLOT-Q capillary column (27.5 m x 0.32 mm) is connected with FID to separate and analyze the products (carrier gas: N_2, flow rate at a minimum: 5 mL/min). The retention time of different chemicals are shown in Table S3 The DMM conversion, products selectivity, and MF STY are calculated as followed:

$$\text{DMM Conv.} = \frac{n_{MF} + n_{DME} + n_{MeOH}}{n_{MF} + n_{DME} + n_{DMM} + n_{MeOH}} \times 100\%$$

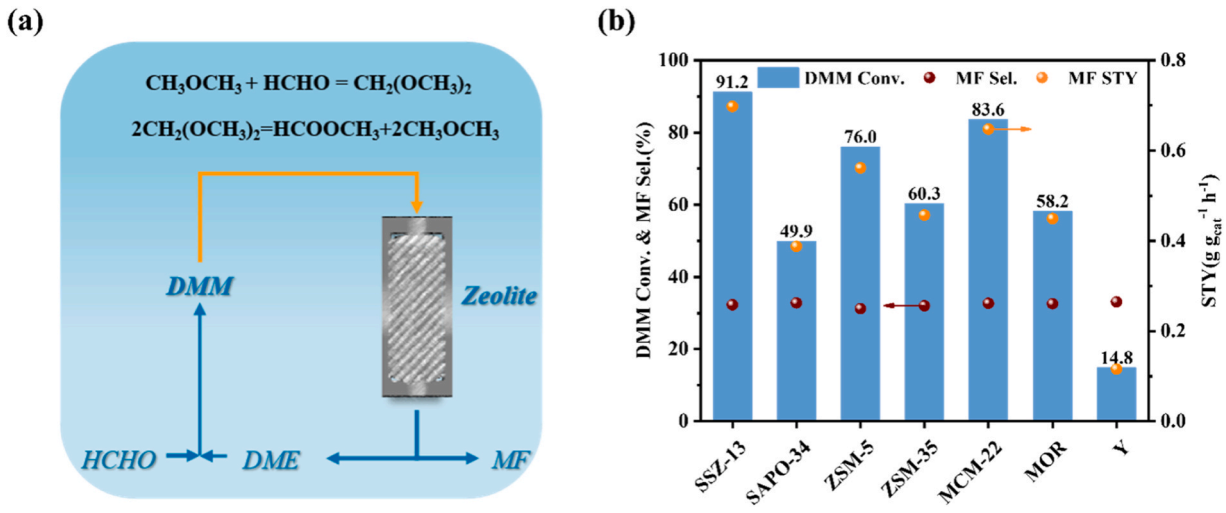

Fig. 1. (a) The diagram of the reaction strategy for MF production; (b) DMM conversion and MF STY over zeolites with different topologies, the theoretical selectivity of MF is 33 %. Reaction conditions: (b) P = 0.1 MPa, T = 373 K, $WHSV_{(DMM)}$ = 2 g g_{cat}^{-1} h^{-1}, $n_{(Ar)}$:$n_{(DMM)}$ = 15:1;.

$$\text{MF Sel.} = \frac{n_{MF}}{n_{MF} + n_{DME} + n_{MeOH}} \times 100\%$$

$$\text{MeOH Sel.} = \frac{n_{MeOH}}{n_{MF} + n_{DME} + n_{MeOH}} \times 100\%$$

$$\text{DME Sel.} = \frac{n_{DME}}{n_{MF} + n_{DME} + n_{MeOH}} \times 100\%$$

$$\text{MF STY} = \frac{\text{DMM Conv.} \times \text{WHSV}_{DMM} \times \frac{3}{2} \times \text{MF Sel.}}{76} \times 60$$

2.4. Temperature program surface reaction (TPSR)

To better understand the mechanism of DMM disproportionation, a TPSR was conducted at 0.1 MPa. Typically, 0.2 g H-SSZ-13 zeolite was loaded in a U-shaped quartz tube and pretreated on 823 K for 60 min in He, then cooled down to room temperature. DMM was introduced into zeolite continuously for 4 h, and then swept by He for 4 h at room temperature. Subsequently, the temperature was increased from room temperature to 573 K with 3 K min^{-1}, and the gas phase was detected by online-MS.

2.5. In situ diffuse reflectance infrared fourier transform spectra (DRIFTs)

In order to further confirmed reaction mechanism, in-situ DRIFT spectra were carried out on a Bruker Tensor 27 instrument equipped with a diffuse reflectance attachment and MCT detector under reaction conditions. Firstly, 20 mg of H-SSZ-13 was placed in the diffuse reflectance infrared cell and calcined in the N_2 (30 mL/min) stream at 673 K for 1 h. Afterward, the catalyst was cooled down to reaction temperature in the N_2 stream. The stream of DMM (0.4 % of DMM and Ar as balance gas) at 30 mL/min was introduced into the cell at 0.1 MPa. Moreover, MF was introduced into the cell by evaporation at 303 K. The spectra were scanned continuously to observe surface species.

2.6. Colorimetric analysis of formaldehyde (FA)

FA was detected by colorimetric analysis during the reaction process and the detailed mechanism is shown in Scheme 1. Before the chromogenic reaction process, the reaction effluents are collected for 5 min by 10 mL absorption liquid which prepared by trolamine, sodium pyrosulfite and EDTA-2Na [35]. Subsequently, 1 mL of above sample is added into glass bottle to detect HCHO, and the following procedure have been summarized in the literature [35]. After 5 min of reaction, the color of the solution is recorded. If the color changes from colorless to purple-red, the existence of HCHO is proved, and the depth of color is correlated with the concentration of HCHO [36].

3. Results and discussion

3.1. Feasibility verification of DMM disproportionation catalyzed by zeolites

To identify the feasibility of our strategy, acidic zeolites with different topologies, including CHA, MFI, FER, MWW, MOR and FAU, were employed as catalysts in the DMM disproportionation. The relative information of structure and physicochemical properties of different zeolites are depicted in Fig. S1 - S3 and Table S4 - S5. These results indicate that all employed zeolites have a typically crystal morphology and high crystallinity without impurities, respectively. Fig. 1(b) exhibits the DMM conversion, MF selectivity and MF STY catalyzed by acidic zeolites with different topologies at 0.1 MPa and 373 K. Obviously, MF could be observed over all the investigated zeolites, which reveals that it is feasible for acidic zeolites to catalyze DMM disproportionation. Although the selectivity of MF over all zeolites are approaching to the theoretical value of 33 %, a significant variation in DMM conversion and the STY of MF could be observed over the different zeolite catalysts. A highest DMM conversion (91.2 %) and MF STY (0.70 g g_{cat}^{-1} h^{-1}) could be observed over H-SSZ-13 among the investigated zeolites. Additionally, different DMM conversion can be obtained over H-ZSM-5 (76.0 %), H-MCM-22 (83.6 %) and H-ZSM-35 (60.3 %), respectively, which all contain 10-membered ring (10-MR). Moreover, the zeolites with 12-MR, including H-MOR and H-Y, exhibit low DMM conversion and MF yield. These results indicate that the topology of the zeolite plays an important role on the DMM disproportionation reaction. On the other hand, different DMM conversion can be found over H-SSZ-13 and H-SAPO-34 with the same topology, respectively. These observations might be owing to the difference on acid strength, as shown in Fig. S3. The results mentioned above indicate that H-SSZ-13 with CHA topology and high acid strength is an excellent catalyst for MF formation. Moreover, the highest MF STY over H-SSZ-13 under the mild conditions indicates that our provided route avoids the drawbacks such as corrosion, high pressure and high temperature for the routes shown in Table S1. Therefore, we can conclude that our strategy about MF production from DMM is feasible, and H-SSZ-13 is proven to be the most efficient catalyst among the zeolites investigated and employed as the preferred catalyst in the following research.

3.2. Effect of reaction conditions on DMM disproportionation

The influence of reaction temperature on DMM disproportionation over H-SSZ-13 has been investigated, as illustrated in Fig. 2(a). With increasing temperature from 333 K to 393 K, DMM conversion and MF STY increase monotonically from 22.3 % to nearly 100 %, and 0.17 g g_{cat}^{-1} h^{-1} to 0.76 g g_{cat}^{-1} h^{-1}, respectively. These results indicate that a higher temperature is beneficial for the formation of MF. As demonstrated in Fig. 2(b), reaction pressure also plays an important role on the DMM disproportionation, the MF STY decreases from 0.70 g g_{cat}^{-1} h^{-1} to 0.42 g g_{cat}^{-1} h^{-1} with increasing pressure from 0.1 MPa to 1 MPa, in agreement with that the equation of DMM disproportionation reaction. Those results reveal that a higher pressure is harmful for DMM disproportionation. On the other hand, a longer contact time facilitates the MF

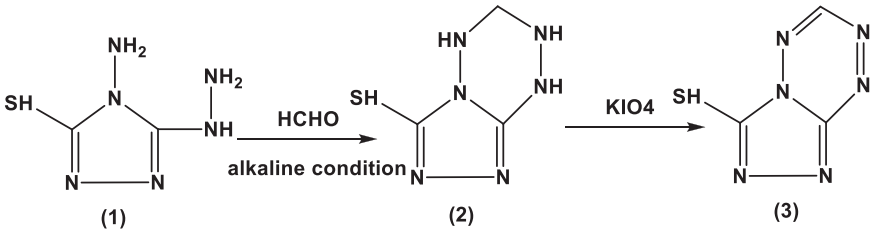

Scheme 1. Colorimetric reaction for HCHO detection. HCHO reacts with compound (1) under alkaline conditions to form compound (2), which is colorless under this condition. Afterwards, the later is oxidized by KIO_4 into compound (3) exhibiting the color of purple-red.

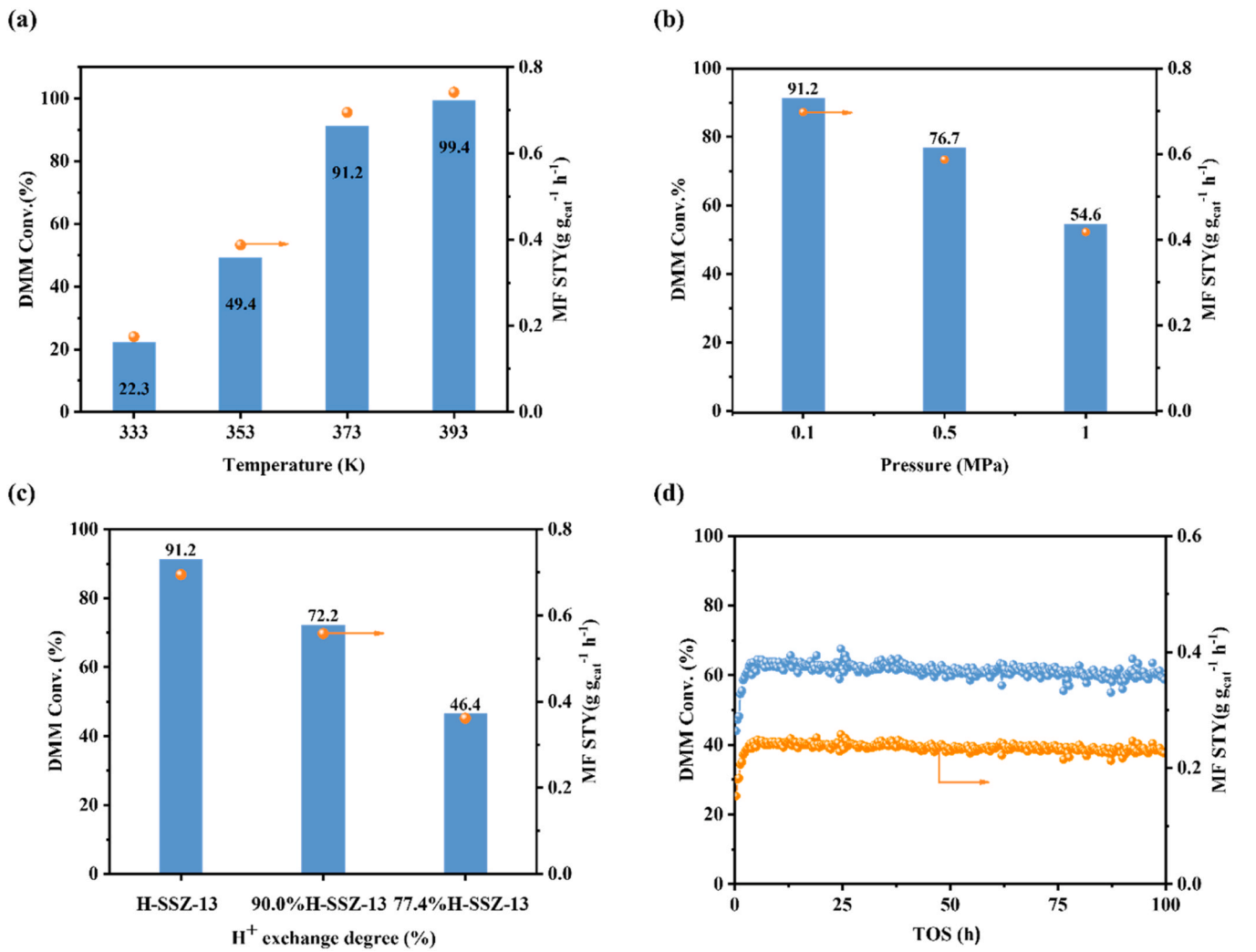

Fig. 2. The effect of (a)reaction temperature; (b) pressure; (c) different H^+ exchange degree on DMM disproportionation over H-SSZ-13; (d) The stability test of DMM disproportionation over H-SSZ-13. Reaction conditions: (a) P = 0.1 MPa, $WHSV_{(DMM)}$ = 2 g g_{cat}^{-1} h^{-1}, $n_{(Ar)}$:$n_{(DMM)}$ = 15:1; (b) T = 373 K, $WHSV_{(DMM)}$ = 2 g g_{cat}^{-1} h^{-1}, $n_{(Ar)}$:$n_{(DMM)}$ = 15:1; (c) P = 0.1 MPa, T = 373 K, $WHSV_{(DMM)}$ = 2 g g_{cat}^{-1} h^{-1}, $n_{(Ar)}$:$n_{(DMM)}$ = 15:1; (d) P = 0.1 MPa, T = 353 K, $WHSV_{(DMM)}$ = 1 g g_{cat}^{-1} h^{-1}, $n_{(Ar)}$:$n_{(DMM)}$ = 15:1.

formation over H-SSZ-13. As shown in Fig. S4, conversion of DMM and MF STY increase from 76.4 % to 100 % and 0.58 g g_{cat}^{-1} h^{-1} to 0.76 g g_{cat}^{-1} h^{-1} respectively, when the contact time is prolonged from 0.44 s to 2.63 s. The acidity of zeolite has an important influence on the catalytic performance. H-SSZ-13 catalysts with different acidity, which are prepared via $NaNO_3$ exchange methods, have been chosen for investigating the influence of acidity.

Fig. 2(c) exhibits the relationship between the catalytic performance of DMM disproportionation and H^+ exchange degree. With decreasing of H^+ exchange, the DMM conversion and MF STY decreases from 91.2 % and 0.70 g g_{cat}^{-1} h^{-1} to 46.4 % and 0.36 g g_{cat}^{-1} h^{-1} respectively. As illustrated in Fig. S5 and Table S6, the amount of acidity decreases with decreasing H^+ exchange degree. These observations demonstrate that the higher amounts of acidic sites are favorable for the formation of MF. Furthermore, γ-Al_2O_3 and Silicalite-1 without BAS were also used as catalysts at 373 K and 0.1 MPa (Table S7). Obviously, no products are observed. Therefore, it can be deduced that the DMM disproportionation is catalyzed by BAS. After optimizing reaction conditions, the stability test has been carried out over H-SSZ-13 at 0.1 MPa and 353 K, as shown in Fig. 2(d), the DMM conversion and MF STY maintain at ca. 63.9 % and 0.24 g g_{cat}^{-1} h^{-1} during 100 h stability test, and the XRD patterns (Fig. S6) demonstrate that the crystallinity of SSZ-13 is almost unchanged after reaction. In summary, an effective and moderate strategy for MF generation can be achieved over H-SSZ-13 from DMM, providing a feasible route for continuous large-scale production for MF.

3.3. *Mechanism of DMM disproportionation over H-SSZ-13*

As shown in Fig. 3(a), an obvious induction period is observed at different reaction temperatures. DMM conversion increases gradually with prolonging the reaction time. Additionally, MF selectivity increases, whereas the selectivity to methanol declines (Fig. S7). Therefore, we speculate that methanol might be originated from the adsorption of DMM along with the formation of surface methoxymethylene species on H-SSZ-13. In order to further identify the reaction mechanism, DRIFTs is conducted at 353 K and 0.1 MPa. Fig. 3(b) displays that the evolution of surface species over H-SSZ-13 with prolonging the reaction time. Two obvious negative peaks at 3736 cm^{-1} and 3664 cm^{-1} are observed, which are assigned to Si-OH and BAS (as shown in Fig. S8), respectively. The intensities of two peaks increase with prolonging the reaction time when DMM is fed on H-SSZ-13. To distinguish the role of Si-OH and BAS in the reaction, Silicalite-1 which only contains Si-OH is also employed as catalyst in our works. Obviously, MF is not detected in the effluent shown in Table S7, demonstrating that Si-OH on Silicalite-1 zeolite cannot catalyze DMM to produce MF. In other words, it can be deduced that the BAS play a

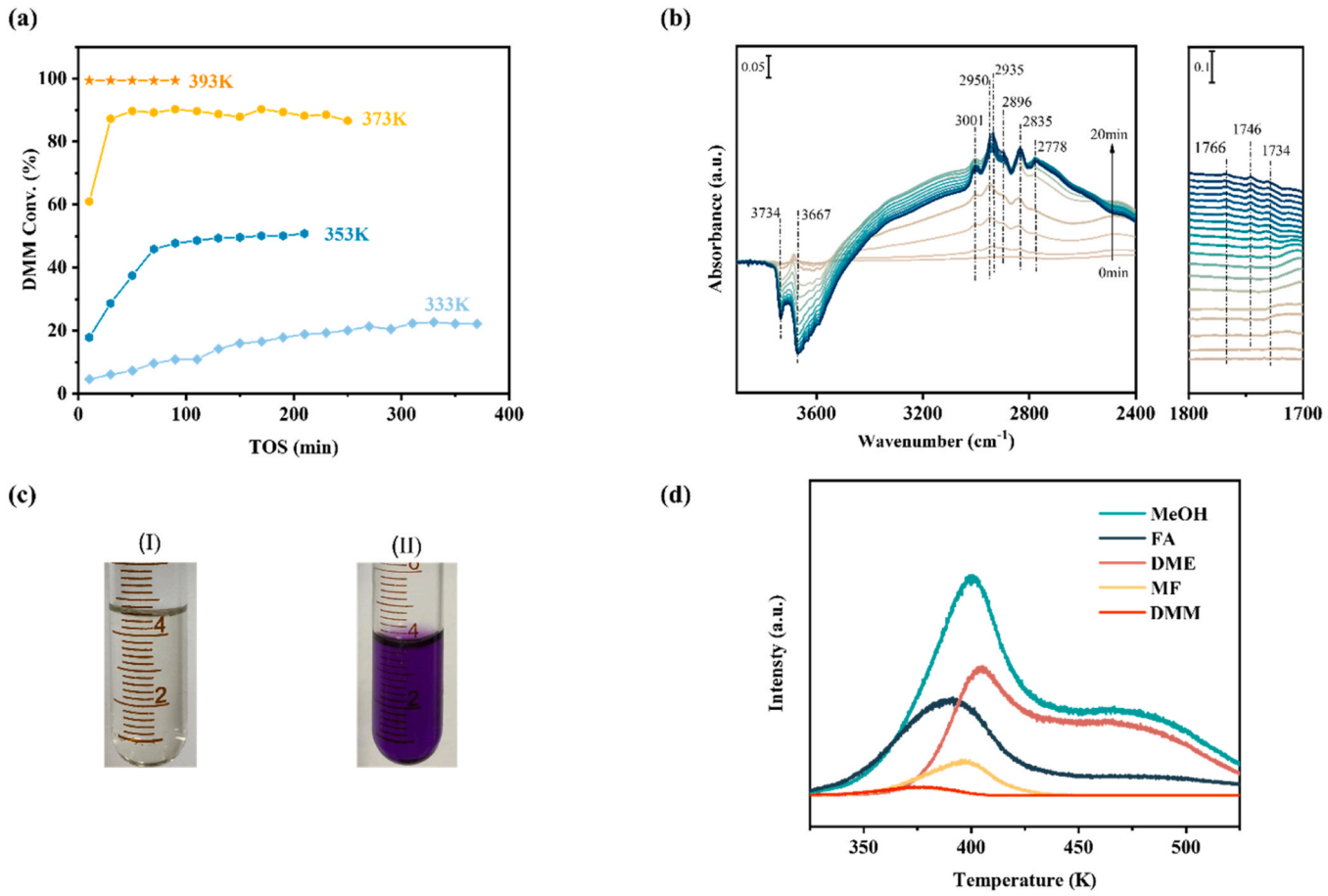

Fig. 3. (a) Changes in DMM conversion during the duration of induction period at different temperature over H-SSZ-13; (b) In situ DRIFT spectra in the DMM disproportionation over H-SSZ-13 with prolonging reaction time; (c) Colorimetric determination results of (I) the contrast sample which DMM, DME, MeOH were added into the absorption liquid and (II) the reaction effusion is collected at steady state; (d)Temperature Programmed Surface Reaction of DMM adsorbed on H-SSZ-13.

determining role on the conversion of DMM whereas the effect of Si-OH over the H-SSZ-13 could be neglected.

The peaks, attributed to the vibration of -CH_3 [20], can be observed at 3001 cm^{-1}, 2950 cm^{-1}, 2835 cm^{-1} and 2778 cm^{-1}. Meanwhile, those assigned to stretching vibration of -CH_2- at 2935 cm^{-1} and 2896 cm^{-1} are found when DMM is introduced into the reaction system. These indicate that methoxymethylene groups are produced originating from DMM absorption over the BAS of H-SSZ-13. Remarkably, the new peak at 1734 cm^{-1} which is ascribed to the C═O bond of FA [37–39] is detected and gradually increased after the appearance of peaks at 2778 cm^{-1} - 3001 cm^{-1}. These suggest that FA can be generated from methoxymethylene groups over the H-SSZ-13, in agreement with the previous reports [36,40–44]. Interestingly, two peaks at 1746 cm^{-1} and 1766 cm^{-1} corresponding the characteristic peaks to the C═O bond of ester are detected in Fig. 3(b). the similar peaks at 1740 cm^{-1} and 1766 cm^{-1} can be observed in Fig. S9 when MF is introduced into H-SSZ-13. These suggest that FA producing from methoxymethylene over the surface of H-SSZ-13 might be converted to MF along with results in the literature [2,45,46]. Therefore, we can deduce that FA should be an important intermediate for the formation of MF.

To further verify the role of FA in the DMM disproportionation, colorimetric analysis of FA has been carried out, as shown in Fig. 3(c). Moreover, the corresponding of DMM conversion and MF STY during the process are depicted in Fig. S10. Obviously, the color of the solution changed to purple gradually in sample (II) of Fig. 3(c), which directly confirms the existence of (FA). Fig. 3(d) exhibits the evolution of effluent with increasing temperature after the adsorption of DMM over H-SSZ-13 detected by mass spectrometry. The signal of DMM is hardly detected, indicating methoxymethylene is formed by chemisorption of DMM. FA and methanol are detected simultaneously at approximately 333 K, and then MF and DME are observed with temperature increasing to 373 K. These results imply that the absorbed methoxymethylene groups are transformed into FA and then converted to MF, which are agreement with in-situ DRIFT.

Based on the mentioned above, we proposed a complete mechanism for DMM disproportionation, as shown in Fig. 4. Specifically, DMM is first adsorbed on BAS forming methoxymethylene group and methanol. Subsequently, the methoxymethylene group is converted to FA and methoxy group. Where into, FA is transformed into MF. Moreover, the methoxy group could reacts with DMM to produce dimethyl ether and methoxymethylene groups.

4. Conclusions

In conclusion, we first develop a green and efficient strategy for directly synthesis of MF via the DMM disproportionation under the heterogeneous catalytic system. H-SSZ-13 presents excellent catalytic performance due to its acidity and unique structure. The BAS over zeolite were found to be the primary active site for DMM conversion. Moreover, the reaction mechanism is proposed which HCHO plays as a key intermediate for MF formation. After optimizing reaction conditions, 0.76 g g_{cat}^{-1} h^{-1} of MF STY is obtained over H-SSZ-13 at 393 K, and displays excellent stability. This strategy with enhanced environmental friendliness and energy efficiency presents a competitive option for

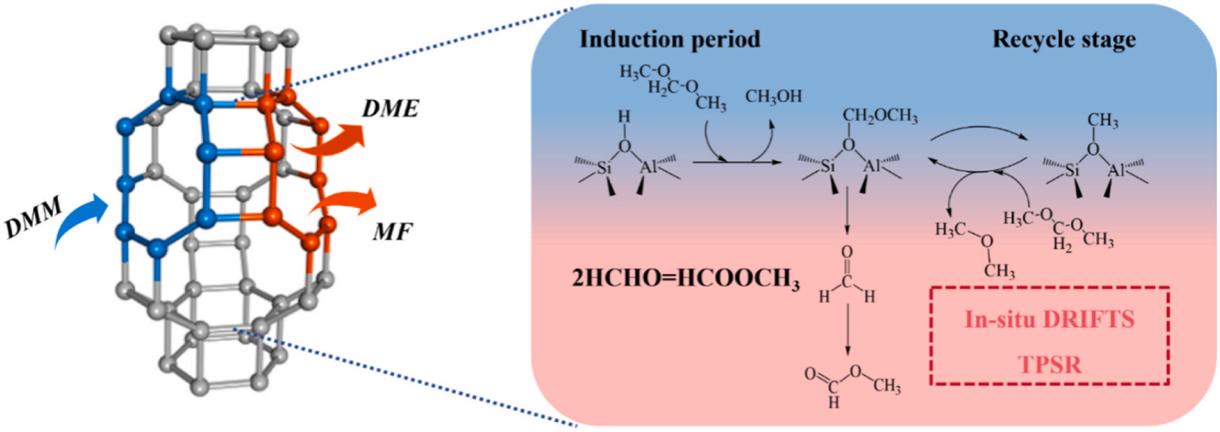

Fig. 4. The proposed mechanism of DMM disproportionation over H-SSZ-13.

large-scale production of MF.

CRediT authorship contribution statement

Leilei Yang: Writing – original draft, Visualization, Validation, Investigation, Conceptualization. **Youming Ni:** Resources, Investigation, Conceptualization. **Mingguan Xie:** Validation, Investigation. **Zhiyang Chen:** Validation, Investigation. **Xudong Fang:** Validation, Investigation. **Bin Li:** Validation, Investigation. **Hongchao Liu:** Visualization, Supervision, Investigation, Conceptualization. **Wenliang Zhu:** Writing – review & editing, Supervision, Conceptualization.

Declaration of Competing Interest

The authors declare that they have no known competing financial interests or personal relationships that could have appeared to influence the work reported in this paper

Data availability

Data will be made available on request.

Acknowledgements

We acknowledge the financial support from the National Natural Science Foundation of China (Grant No. 22378388, 21991094 and 21991090), and the Strategic Priority Research Program of the Chinese Academy of Sciences (Grant No. XDA29030401, XDA21030100), and the Dalian High Level Talent Innovation Support Program (2017RD07), and National Special Support Program for High Level Talents (SQ2019RA2TST0016).

Appendix A. Supporting information

Supplementary data associated with this article can be found in the online version at doi:10.1016/j.apcata.2024.119860.

References

[1] L. Rong, Z. Xu, J. Sun, G. Guo, New methyl formate synthesis method: coal to methyl formate, J. Energy Chem. 27 (2018) 238–242.
[2] D. Kaiser, L. Beckmann, J. Walter, M. Bertau, Conversion of green methanol to methyl formate, Catalysts 11 (2021) 869.
[3] Marco Di Girolamo, M. Marchionna, Acidic and basic ion exchange resins for industrial applications, J. Mol. Catal. Chem. 177 (2001) 33–40.
[4] S. Jali, H.B. Friedrich, G.R. Julius, The effect of $Mo(CO)_6$ as a co-catalyst in the carbonylation of methanol to methyl formate catalyzed by potassium methoxide under CO, syngas and H_2 atmospheres. HP-IR observation of the methoxycarbonyl intermediate of $Mo(CO)_6$, J. Mol. Catal. Chem. 348 (2011) 63–69.
[5] E. GeÂrard, H. GoÈtz, S. Pellegrini, Y. Castanet, A. Mortreux, Epoxide-tertiary amine combinations as efficient catalysts for methanol carbonylation into methyl formate in the presence of carbon dioxide, Appl. Catal. A-Gen. 170 (1998) 297–306.
[6] D.J. Darensbourg, R.L. Gary, C. Ovalles, M. Pala, Homogeneous catalysis of methyl formate production from carbon monoxide and methanol in the presence of metal carbonyl catalysts, J. Mol. Catal. 29 (1985) 285–290.
[7] T. Sodesawa, Dehydrogenation of methanol to methyl formate over Cu-SiO_2 catalysts prepared by ion exchange method, React. Kinet. Catal. Lett. 102 (1986) 460–463.
[8] D.J. Yuan, A.M. Hengne, Y. Saih, K.W. Huang, Nonoxidative dehydrogenation of methanol to methyl formate through highly stable and reusable CuMgO-based catalysts, ACS Omega 4 (2019) 1854–1860.
[9] R. Wojcieszak, A. Karelovic, E.M. Gaigneaux, P. Ruiz, Oxidation of methanol to methyl formate over supported Pd nanoparticles: insights into the reaction mechanism at low temperature, Catal. Sci. Technol. 4 (2014) 3298–3305.
[10] V.V. Kaichev, G.Y. Popova, Y.A. Chesalov, A.A. Saraev, D.Y. Zemlyanov, S. A. Beloshapkin, A. Knop-Gericke, R. Schlögl, T.V. Andrushkevich, V.I. Bukhtiyarov, Selective oxidation of methanol to form dimethoxymethane and methyl formate over a monolayer V_2O_5/TiO_2 catalyst, J. Catal. 311 (2014) 59–70.
[11] W. Kemi, M. Berger, J. Schlupp, High-pressure homogeneous hydrogenation of carbon monoxide in polar and nonpolar solvents, J. Catal. 61 (1979) 359–365.
[12] H.J. Zhao, M.G. Lin, K.G. Fang, J. Zhou, Y.H. Sun, Preparation and evaluation of Cu-Mn/Ca-Zr catalyst for methyl formate synthesis from syngas. Appl. Catal. A-Gen. 514 (216) 276-283.
[13] J.J. Corral-Pérez, A. Bansode, C.S. Praveen, A. Kokalj, H. Reymond, A. Comas-Vives, J. VandeVondele, C. Copéret, P.R. von Rohr, A. Urakawa, Decisive role of perimeter sites in silica-supported ag nanoparticles in selective hydrogenation of CO_2 to methyl formate in the presence of methanol, J. Am. Chem. Soc. 140 (2018) 13884–13891.
[14] C.F. Li, X.Z. Yang, G.J. Gao, Y.Y. Li, W.D. Zhang, X.T. Chen, H.Q. Su, S.J. Wang, Z. Wang, Copper on the inner surface of mesoporous TiO_2 hollow spheres: a highly selective photocatalyst for partial oxidation of methanol to methyl formate, Catal. Sci. Technol. 9 (2019) 6240–6252.
[15] G.A. Filonenko, W.L. Vrijburg, E.J. Hensen, E.A. Pidko, On the activity of supported Au catalysts in the liquid phase hydrogenation of CO_2 to formates, J. Catal. 343 (2016) 97–105.
[16] W. Wang, X. Gao, R. Feng, Q. Yang, T. Zhang, J. Zhang, Q. Zhang, Y. Han, Y. Tan, Hierarchical H-MOR zeolite supported vanadium oxide for dimethyl ether direct oxidation, Catalysts 9 (2019) 289–297.
[17] C.F. Breitkreuz, N. Hevert, N. Schmitz, J. Burger, H. Hasse, Synthesis of methylal and poly(oxymethylene) dimethyl ethers from dimethyl ether and trioxane, Ind. Eng. Chem. Res. 61 (2022) 7810–7822.
[18] F.E. Celik, T.J. Kim, A.T. Bell, Vapor-phase carbonylation of dimethoxymethane over H-Faujasite, Angew. Chem. Int. Ed. 48 (2009) 4813–4815.
[19] F.E. Celik, T. Kim, A.N. Mlinar, A.T. Bell, An investigation into the mechanism and kinetics of dimethoxymethane carbonylation over FAU and MFI zeolites, J. Catal. 274 (2010) 150–162.
[20] F.E. Celik, T.J. Kim, A.T. Bell, Effect of zeolite framework type and Si/Al ratio on dimethoxymethane carbonylation, J. Catal. 270 (2010) 185–195.
[21] J. Yao, Y. Wang, S.S. Bello, G. Xu, L. Shi, Regulation of Brønsted acid sites in H-MOR for selective methyl methoxyacetate synthesis, Appl. Organomet Chem. 34 (2020) e5925.
[22] F. Chen, D. Zhang, L. Shi, Y. Wang, G. Xu, Optimized pore structures of hierarchical HY zeolites for highly selective production of methyl methoxyacetate, Catalysts 9 (2019) 865.
[23] F. Chen, L. Shi, S. Bello, J. Fan, Y. Wang, D. Zhang, J. Yao, Excellent prospects in methyl methoxyacetate synthesis with a highly active and reusable sulfonic acid resin catalyst, New J. Chem. 44 (2020) 1346.
[24] D.X. Zhang, L. Shi, Y. Wang, F. Chen, J. Yao, X.Y. Li, Y.M. Ni, W.L. Zhu, Z.M. Liu, Effect of mass-transfer control on HY zeolites for dimethoxymethane carbonylation to methyl methoxyacetate, Catal. Today 316 (2018) 114–121.

[25] Z. Xie, C. Chen, B. Hou, D. Sun, H. Guo, J. Wang, D. Li, L. Jia, Study of the nature of high-silica H–Y acid sites in dimethoxymethane carbonylation by NH_3 poisoning, J. Phys. Chem. C 122 (2018) 9909–9917.
[26] J. Yao, L. Shi, W. Deng, J. Fan, Y. Wang, W. Gao, D. Zhang, W. Zhu, Z. Liu, Facile sulfolane-modified resins for enhanced dimethoxymethane carbonylation, Catal. Sci. Technol. 10 (2020) 2561–2572.
[27] Y. Li, L. Li, J.H. Yu, Applications of zeolites in sustainable chemistry, Chem 3 (2017) 928–949.
[28] P. Tian, Y.X. Wei, M. Ye, Z.M. Liu, Methanol to olefins (MTO): from fundamentals to commercialization, ACS Catal. 5 (2015) 1922–1938.
[29] P. Cheung, A. Bhan, G.J. Sunley, E. Iglesia, Selective carbonylation of dimethyl ether to methyl acetate catalyzed by acidic zeolites, Angew. Chem. Int. Ed. 45 (2006) 1617–1620.
[30] K.P. Cao, D. Fan, L.Y. Li, B.H. Fan, L.Y. Wang, D.L. Zhu, Q.Y. Wang, P. Tian, Z. M. Liu, Insights into the pyridine-modified MOR zeolite catalysts for DME carbonylation, ACS Catal. 10 (2020) 3372–3380.
[31] J. Becher, D.F. Sanchez, D.E. Doronkin, D. Zengel, D.M. Meira, S. Pascarelli, J. D. Grunwaldt, T.L. Sheppard, Chemical gradients in automotive Cu-SSZ-13 catalysts for NO_x removal revealed by operando X-ray spectrotomography, Nat. Catal. 4 (2021) 46–53.
[32] E. Borfecchia, P. Beato, S. Svelle, U. Olsbye, C. Lamberti, S. Bordiga, Cu-CHA - a model system for applied selective redox catalysis, Chem. Soc. Rev. 47 (2018) 8097–8133.
[33] S. Asthana, C. Samanta, A. Bhaumik, B. Banerjee, R.K. Voolapalli, B. Saha, Direct synthesis of dimethyl ether from syngas over Cu-based catalysts: enhanced selectivity in the presence of MgO, J. Catal. 334 (2016) 89–101.
[34] A. Ghosh, D. Nag, R. Chatterjee, A. Singh, P.S. Dash, Biswajit Choudhury, Asim Bhaumik, CO_2 to dimethyl ether (DME): structural and functional insights of hybrid catalysts, Catal. Sci. Technol. 14 (2024) 1387–1427.
[35] GB/T 16129-1995
[36] S. Lin, Y. Zhi, W. Zhang, X. Yuan, C. Zhang, M. Ye, S. Xu, Y. Wei, Z. Liu, Hydrogen transfer reaction contributes to the dynamic evolution of zeolite-catalyzed methanol and dimethyl ether conversions: Insight into formaldehyde, Chin. J. Catal. 46 (2023) 11–27.
[37] G.Y. Popova, A.Y. Chesalov, T.V. Andrushkevich, E.S. Stoyanov, Heterogeneous selective oxidation of formaldehyde on oxide catalysts: in situ ftir study of formaldehyde surface species on a V-Ti-O catalyst and oxygen effect, Kinet. Catal. 41 (2000) 546–552.
[38] S. Müller, Y. Liu, F.M. Kirchberger, M. Tonigold, M. Sanchez-Sanchez, J.A. Lercher, Hydrogen transfer pathways during zeolite catalyzed methanol conversion to hydrocarbons, J. Am. Chem. Soc. 138 (2016) 15994–16003.
[39] Y. Liu, F.M. Kirchberger, S. Müller, M. Eder, M. Tonigold, M. Sanchez-Sanchez, J. A. Lercher, Critical role of formaldehyde during methanol conversion to hydrocarbons, Nat. Commun. 10 (2019) 1462.
[40] A.K. Kolah, S.M. Mahajani, M.M. Sharma, Acetalization of formaldehyde with methanol in batch and continuous reactive distillation columns, Ind. Eng. Chem. Res. 35 (1996) 3707–3720.
[41] W. Ahmad, F.L. Chan, A.L. Chaffee, H. Wang, A. Hoadley, A. Tanksale, Dimethoxymethane production via catalytic hydrogenation of carbon monoxide in methanol media, ACS Sustain. Chem. Eng. 8 (2020) 2081–2092.
[42] Z.H. Wei, Y.Y. Chen, J.F. Li, P.F. Wang, B.Q. Jing, Y. He, M. Dong, H.J. Jiao, Z. F. Qin, J.G. Wang, W.B. Fan, Methane formation mechanism in the initial methanol-to-olefins process catalyzed by SAPO-34, Catal. Sci. Technol. 6 (2016) 5526–5533.
[43] F.M. Kirchberger, Y. Liu, P.N. Plessow, J.A. Lercher, Mechanistic differences between methanol and dimethyl ether in zeolite-catalyzed hydrocarbon synthesis, Proc. Natl. Acad. Sci. U. S. A. 119 (2022) e2103840119.
[44] P.N. Plessow, F. Studt, Unraveling the mechanism of the initiation reaction of the methanol to olefins process using ab initio and DFT calculations, ACS Catal. 7 (2017) 7987–7994.
[45] L. Domokos, T. Katona, A. Molmnar, Dehydrogenation of methanol to methyl formate: deuterium labeling studies, Catal. Lett. 40 (1996) 215–221.
[46] E. Miyazaki, I. Yasumor, Kinetics of the catalytic decomposition of methanol, formadehyde and methyl formate over a copper-wire surface, Bull. Chem. Soc. Jpn. 40 (1967) 2012–2017.